ELSEVIER

Surface Science 401 (1998) 162–172

surface science

The termination of the α-Al_2O_3 (0001) surface: a LEED crystallography determination

J. Toofan, P.R. Watson *

Department of Chemistry, Oregon State University, Gilbert Hall 153, Corvallis, OR 97331, USA

Received 15 July 1997; accepted for publication 25 November 1997

Abstract

We have performed a tensor low-energy electron diffraction (TLEED) determination of 10 diffracted beams at off-normal incidence from the (0001) surface of α-Al_2O_3 produced by oxygen plasma cleaning/annealing cycles. Structures with single domain O- or Al-terminated surface layers give a poor agreement (Pendry R-factor = 0.42). Such domains are related by steps in the $(11\bar{2}0)$ direction that produce an extra plane of symmetry in the LEED pattern. Allowing a mixture of domains due to steps produces a good agreement. An optimized mixture of 2:1 O/Al-terminated domains lowers the R-factor to 0.26 with an inner potential of 19.2 eV. At the R-factor minimum, we find that in both domains, the outermost atomic layer relaxes outward, with some twisting and relief of buckling in deeper layers. An outward relaxation of the top layer is in disagreement with theoretical predictions. However, such predictions are for vacuum-cleaved surfaces that are not realistic descriptions of the surface used in our experiment.

Keywords: Alumina surfaces; Crystallography; LEED; Surface structure; α-Al_2O_3(0001)

1. Introduction

The corundum modification of alumina (α-Al_2O_3) is an important material with applications as optical windows, masers and in thin-film microelectronics applications. The surface chemistry of the principal growth planes, particularly the c-plane (0001), of this material have been extensively studied with the surprising exception that the surface structures have not been experimentally determined. LEED studies of the (0001) surface have been made by several workers [1–4]. In general, a surface freshly etched in phosphoric acid yields a poor (1×1) pattern. Heating to about 1300 K improves the pattern. Further heating to 1300–1700 K produces a complex $(\sqrt{31}\times\sqrt{31})$R9° pattern resulting from loss of oxygen from the surface. Heating in oxygen restores the (1×1) pattern. Other metastable structures such as $(\sqrt{3}\times\sqrt{3})$R30° have also been observed [2]. Intensity–voltage – $I(V)$ – curves for the specular beam at various incidence angles were reported by Wei and Smith [4], but no surface crystallographic determination using modern LEED methods has been reported.

The surface of an alumina (0001) crystal can terminate in several ways, and there have been a number of calculations aimed at predicting the most stable alumina surfaces [5–8]. These uniformly predict the (1×1) Al_2O_3 (0001) surface to

* Corresponding author. Fax: (+1) 503 737 2062.

0039-6028/98/$19.00
PII: S0039-6028(97)01031-5

be terminated with a layer of Al atoms and show significant displacements of surface atoms from bulk positions.

We have recorded extensive LEED $I(V)$ data for (1×1) Al_2O_3 (0001) at off-normal incidence and compared these data with theoretical $I(V)$ curves produced using the latest tensor LEED (TLEED) [9] codes. These codes perform a directed search for the structure that best fits the experimental data allowing the coordinates of all the atoms in the surface unit cell to relax from a trial structure. We find that both Al- and O-terminated surfaces show a reasonable agreement with the experimental data.

2. Bulk structure of α-Al_2O_3

The bulk structure of the α-modification of alumina is sufficiently complex such that it is appropriate to first conduct a brief review of the situation in the bulk before considering the surface properties. Bulk α-Al_2O_3 (space group: $R\bar{3}c$) can be described as a hexagonal unit cell containing six formula units. It is also frequently described by a rhombohedral unit cell containing two formula units of Al_2O_3. For interionic distance calculations, use is often made of yet a different unit cell that is rectangular rather than rhombohedral or hexagonal. Such a cell is classified [10] as orthohexagonal. For our purposes, the hexagonal cell is convenient. The structure of α-Al_2O_3 is closely related to the ideal corundum structure ($c/a=2\sqrt{2}$) shown in Fig. 1. Here, the Al^{3+} ions lie along the c-axis in coplanar layers, filling 2/3 of the octahedral holes between layers of O^{2-} ions. These oxide layers are equidistant from each other, spaced 1/6 of the unit cell side c apart. In this idealized structure, the Al^{3+} ions ($u=1/2$) are situated halfway between two oxide layers. In the oxygen layers themselves, the O^{2-} ions ($v=1/3$) are equidistant from each other, forming an exactly hexagonal arrangement.

In reality, the Al^{3+} ions in Al_2O_3 do not form coplanar layers but are buckled as shown in Fig. 2. As a result, the two neighboring oxide layers to each Al^{3+} ion are located at different distances, as can be clearly seen in the cross-section shown in Fig. 3b. This displacement divides the six nearest-neighbor oxygen ions into two triads of equivalent ions located in two adjacent layers. In the oxide layers, the O^{2-} ions are also slightly shifted

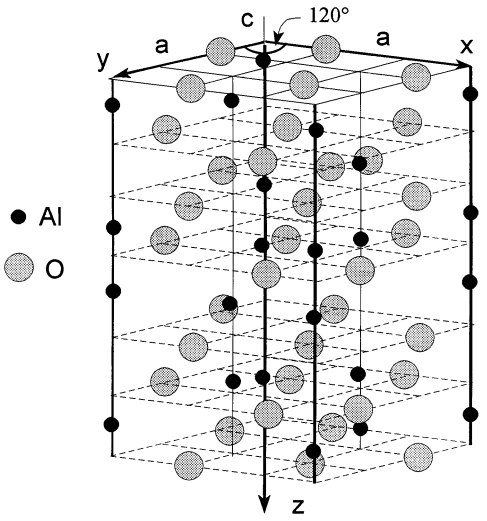

Fig. 1. Idealized corundum structure ($u=1/2$, $v=1/3$) for alumina showing the locations of the aluminum and oxygen ions in the hexagonal unit cell. The angle between the x- and y-axes is 120°. The aluminum ions are located on the heavy vertical lines, while the oxygen ions are located at the intersections of the horizontal (dashed) lines.

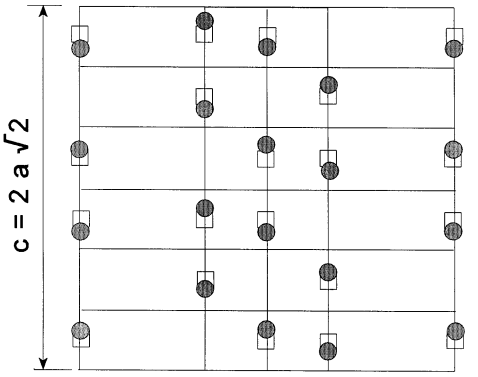

Fig. 2. Cross-section of the idealized (□) and real (·) arrangement of aluminum ions in the hexagonal unit cell of alumina. The value of $c=2a\sqrt{2}$ is used for the idealized structure. The aluminum ions in the ideal structure are coplanar, but in the real structure are in buckled layers.

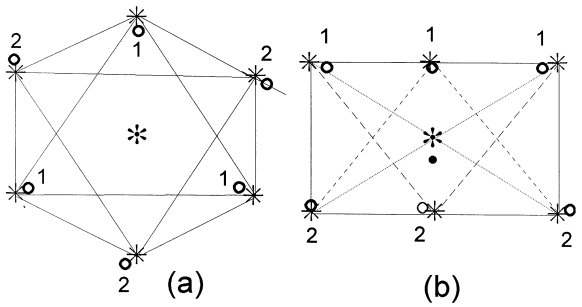

Fig. 3. Top (a) and cross-setion (b) of a set of O–Al–O layers in the ideal and real alumina hexagonal unit cell showing the octahedron of nearest O neighbors [idealized (∗) and real (◦) case] to an Al ion [idealized (∗) and real (·) case].

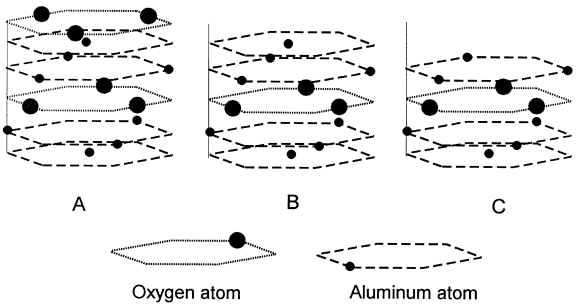

Fig. 4. Three possible surface terminations of the alumina (0001) surface that lead to crystallographically distinct surfaces A, O-terminated; B, Al-bilayer terminated; C, Al-terminated. Each surface can be obtained from the previous one by removing a layer of O or Al ions.

laterally away from the ideal positions. In the O^{2-} layer furthest from the Al^{3+} ion, each triad of oxide ions shrinks evenly towards the *c*-axis. In the other layer, closest to the Al^{3+} ion, each triad is expanded and twisted about the *c*-axis (see Fig. 3a).

For unit cell parameters, we have used the recent synchrotron data of Thompson et al. [11] who reported $a=4.759$ Å, $c=12.990$ Å and $u=0.352$, $v=0.692$.

3. Surface termination of α-Al_2O_3

In most simple binary oxides, the (1×1) structure, where known [12], is close to a simple truncated bulk structure. If we assume that the surface structure of alumina is based on a truncation of the bulk structure, then there are three obvious simple model reference structures to investigate that differ with respect to termination. These are shown in Fig. 4. In termination A, the last layer in the surface is an O layer. Removing just this layer yields a structure B that is terminated by an Al-bilayer. Structure C is an Al-termination resulting from removal of the top Al layer from B. The layout of the surface unit cell for the A-termination is shown in Fig. 5.

The influence of steps is interesting. An unstepped surface of a certain termination will only possess a threefold symmetry axis. Because of the absence of any mirror planes of symmetry

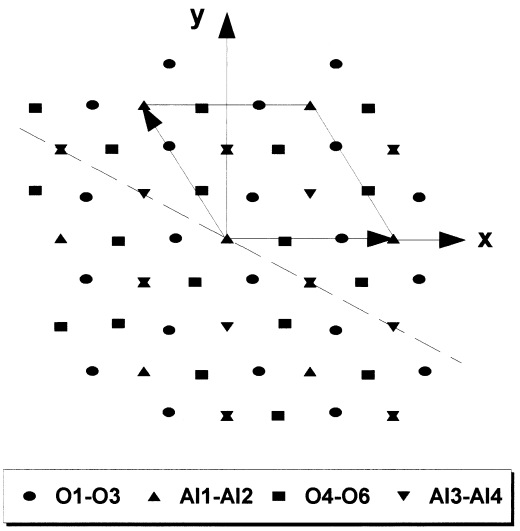

Fig. 5. View down the C_3 axis of the atoms in the O-terminated A reference structure. The dashed line represents a mirror plane of symmetry introduced by steps (see text). The coordinates of the atoms are given in Table 1.

in the alumina structure, the LEED pattern at off-normal incidence should not have any diffraction beams that are related by symmetry. However, any two (0001) surfaces with the same termination but differing in thickness by $(c/6)=2.16$ Å (equivalent to one Al–O–Al sandwich) are equivalent to each other via a mirror reflection about the $(11\bar{2}0)$ plane (see Fig. 5). Steps of this type on an (0001) surface will mix LEED beams from different terraces within the LEED coherence area.

In general, this will not lead to new symmetries between beams unless the electron beam is incident along the step direction ($11\bar{2}0$), in which case pairs of symmetrically-related beams will result.

4. Experimental details

Single crystals of Al_2O_3 (0001), with dimensions of $10 \times 10 \times 0.5$ mm and polished one side, were purchased from Johnson Matthey Alfa Aesar. After pre-cleaning with acetone and methanol, a back-reflection Laue camera was used to determine any misorientation with the aid of a Greninger net. Samples could be misaligned by as much as 1.8°. It is commonly found that commercial sapphire crystals are miscut to some degree. The crystal was cleaned ultrasonically in acetone and rinsed with pure methanol and dried with flowing nitrogen. About 4000 Å of β-tantalum were sputtered (in a 90% Ar and 10% N_2 atmosphere) on to the unpolished face to provide a high electrical conductivity path for resistive heating [13]. The polished face of the crystal was also covered with Ta except for a window with a diameter of 6.0 mm at the center of crystal. The surface Ta film also serves to help reduce surface charging as well as being used for resistive heating. The crystal was clamped in a wing-shaped piece of tantalum metal (0.025 mm thick), and the sides of the wing were fixed between grooves in the Ta bars of holder (Fig. 6). A W/Re thermocouple was attached to the surface, at the top of the clear window, with a high-temperature ceramic adhesive. After cleaning, the holder was mounted on a manipulator in a UHV system equipped with LEED/Auger hemispherical electron optics. The system was located inside a cubic Helmholtz coil to reduce the influence of external magnetic fields.

After baking to 120°C for 48 h with an external molecular drag pump running, the pressure dropped to 5×10^{-5} Torr after the temperature of the chamber had returned to 60°C. One day after baking, using the ion pump in parallel with a Ti-sublimation pump, the pressure dropped to the stable 2.0×10^{-9} Torr range. The sample initially was heated resistively using a temperature programmer to 500°C. We then injected oxygen

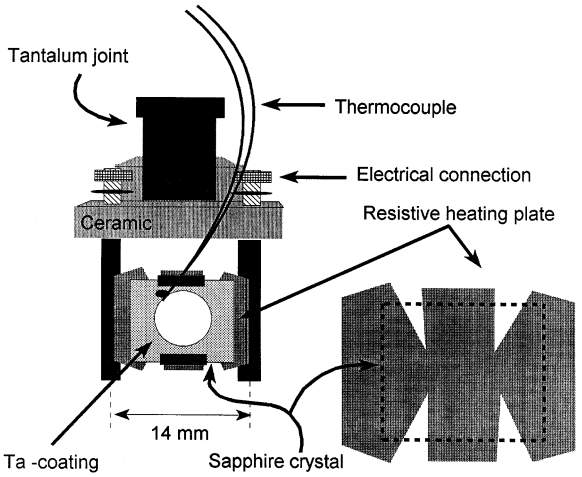

Fig. 6. Alumina sample holder. The maximum heat is produced in the center of the resistive heating tantalum plate (the dashed line square shows the position of the sample), where it contacts the area of the back of the clear window on the sample.

into the chamber for 2 min ($p = 10^{-4}$ Torr) and switched on a Tesla coil connected to the head of the high voltage electrical feedthrough for 3 min to oxidize carbon contamination on the surface via an oxygen plasma [14]. The process of cleaning was monitored by taking an AES spectrum and measuring the size of the carbon peak [15] and repeated until no further change occurred. In the final stages of the cleaning, we found that there was a trace of carbon on the spectrum that could not be removed under our conditions (Fig. 7).

After a final cleaning of the sample by exposing it to an oxygen plasma (2.5×10^{-6} Torr for 1.0 min) and resistive heating (850°C for 3.0 min), the sample was arranged to face the LEED/Auger optics again. We experienced considerable difficulty with charging when attempting to observe LEED patterns. Depending upon the degree of charging, the pattern could be distorted and an aurora-type phenomenon appeared on the LEED screen. After much trial and error, it was found that the most effective way to reduce charging effects was to focus the LEED beam close to the edge of the clear window on the specimen close to the surrounding Ta film. This tactic apparently allows charge to drain effectively from the sample. Starting from a low energy, we were restricted to a minimum of 78 eV under our conditions. If we

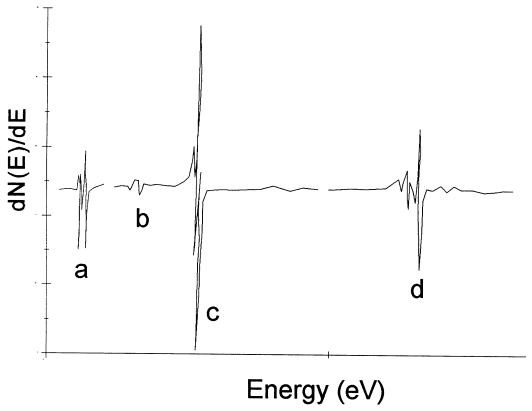

Fig. 7. Auger spectrum of α-Al_2O_3 after oxygen plasma cleaning. The various regions of the spectrum represent (a) Al *LVV* (~56 eV); (b) C *KLL* (~270 eV); (c) O *KVV* (~506 eV); and (d) Al *KLL* (~1366 eV). The trace of carbon on the surface decreased during cleaning but was not removed completely. The absolute positions of peaks depend upon the degree of surface charging.

changed the electron energy inversely (from high to low energy), the lowest attainable energy at which diffraction could be observed due to charging was about 58 eV. The main effect of charging under these conditions is to shift the zero of the voltage scale in the $I(V)$ curves. Fortunately, this quantity is effectively a parameter to be determined by shifts in the inner potential used in the calculations and so is not a cause of concern.

One result of charging that was of more concern was that in order to observe stable LEED patterns, we were unable to work at normal incidence. Most LEED studies occur at normal incidence to cut down on the computational complexity. We were forced by circumstances to carry out long computations associated with off-normal incidence, but this actually turned out to have a beneficial side-effect. The polar angle of the incident beam with respect to the surface normal, θ, and azimuthal angle between the crystal x-axis and the projection of the incident beam on the crystal surface, ϕ, were found using the method of Cunningham and Weinberg [16] to be $\theta = 8.8^\circ$ and $\phi = -31.0^\circ$. This azimuthal angle is coincidentally very close to the step direction ($\phi = -30.0^\circ$) as shown in Fig. 5.

We observed three types of LEED pattern. Heating to less than 750°C produced a (1×1)

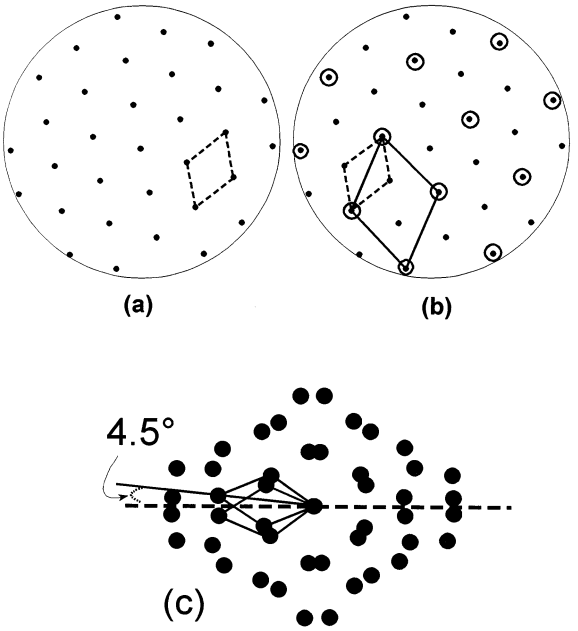

Fig. 8. Representation of two diffraction patterns observed on (0001) aluminum oxide crystal (a) (1×1), and (b) $(\sqrt{3} \times \sqrt{3})R \pm 30^\circ$; (c) exploded view of a part of the coincidence lattice $(\sqrt{31} \times \sqrt{31})R \pm 9^\circ$ pattern found upon heating to above 1200°C.

LEED pattern (Fig. 8a). Heating further to less than a 1000°C resulted in a weak $(\sqrt{3} \times \sqrt{3})R30^\circ$ pattern (Fig. 8b). Further heating beyond 1100°C yielded the complex pattern shown in Fig. 8c and was indexed as $(\sqrt{31} \times \sqrt{31}) \pm \tan(\sqrt{3/11})$. The (1×1) pattern was regained by cooling the $(\sqrt{31} \times \sqrt{31})$ structure in oxygen. Subsequent heat treatments for 2 min at 750°C improve the intensity and sharpness of the (1×1) pattern. These observations are consistent with those described in the literature [1–4].

Images of the moderately sharp (1×1) pattern were recorded at 303 K using a computer-controlled video camera/image capture board (Oculus 200) over an energy range of 80–190 eV at 2 eV intervals. These images were stored directly on the hard disk of the computer. The recording time was less than 10 min per dataset. Several sets of data with different sample positions and camera gain adjustments were collected and stored. Sets of stored data were analyzed using a new image processing program [17] to extract $I(V)$ curves.

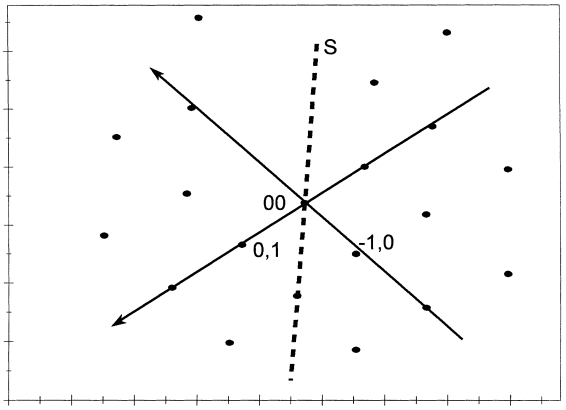

Fig. 9. Experimental positions of 20 spots in (1×1) LEED pattern from the (0001) surface of α-Al_2O_3 at $\theta=8.8^\circ$ and $\phi=-31.0^\circ$, showing the reciprocal lattice vectors. The dashed line shows the symmetry plane present due to steps (see text).

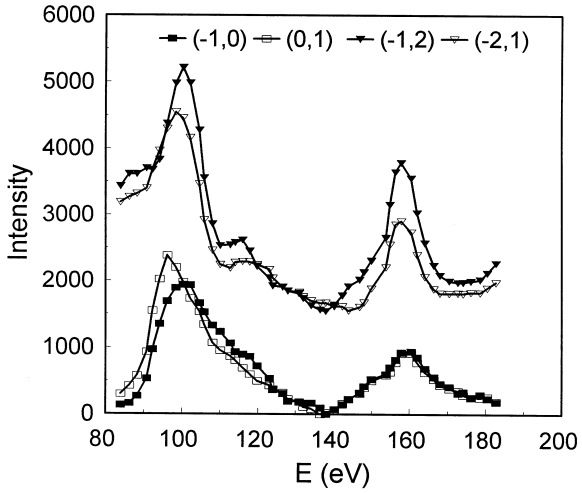

Fig. 10. $I(V)$ curves from two symmetrically related sets of experimental beams from alumina (0001).

The $I(V)$ curves of the 20 beams shown in Fig. 9 were recorded.

Examination of these off-normal $I(V)$ curves (Fig. 10) indeed revealed the presence of a extra plane of symmetry (Fig. 9) in the pattern resulting from incidence along the step direction that produces averaged contributions from domains related by a $(c/6)$ step as detailed earlier. Fig. 10 shows that the (1,0) and $(0,\bar{1})$, $(\bar{1},2)$ and $(\bar{2},1)$, and other pairs of beams are clearly symmetry-related. After rejecting beams with energy ranges that were too short or that were excessively noisy, we were left with a set of 10 beams from the original set of 20 beams that were used in the structure determination. The total energy range of all the beams was 1000 eV.

5. Calculations

LEED calculations need atomic phase shifts as a function of angular momentum. Although values are tabulated for elements, phase shifts do vary with oxidation state and the structure of the solid. We recalculated Al and O phase shifts for the Al_2O_3 structure for both neutral and ionic atoms using the phase-shift programs supplied in the TLEED package [9]. The value of the exchange parameter in the SCF-Xα method was obtained from Ref. [18]. Other initial parameters for the LEED calculation were:

$V_{or}=20.0$ eV, $V_{oi}=-6.0$ eV;

$\theta_D(\mathrm{Al})=420$ K, $\theta_D(\mathrm{O})=1217$ K.

For primary energies above 90 eV, the shapes of the resulting $I(V)$ curves and the resulting R-factors were less sensitive to the details of the construction of the phase shifts – the muffin-tin radii, exchange parameter and starting wavefunctions (ionic or neutral atom) – than to small changes in the structural model. Some problems with non-convergence occurred at very low energies when purely ionic occupation of the atomic orbitals was used in the phase shifts calculation.

The oxygen and aluminum atoms were organized in terms of composite layers that contain more than one atom per two-dimensional unit cell. The crystal is built up of such composite layers containing up to 10 atomic sublayers each (sublayers can be coplanar). The surface contains 10 symmetrically distinct atomic sublayers arranged in six physical layers for the A reference structure; seven atoms in five physical layers for termination B; and six atoms in four physical layers for termination C (see Fig. 4 and Table 1). The bulk crystal was constructed of three repeats of an A-type termination with appropriate offsets. The presence of the extra symmetry induced by steps means that symmetrically equivalent pairs of

Table 1
Coordinates used for the O-terminated alumina (0001) reference structure A[a]

Atom	Δx (Å)	Δy (Å)	Δz (Å)
O1	−1.4685	0.0000	0.0000
O2	0.7343	−1.2718	0.0000
O3	0.7343	1.2718	0.0000
Al1	2.3793	−1.3737	0.8426
Al2	0.0000	0.0000	1.3224
O4	1.6540	−0.1019	2.1650
O5	1.6540	−2.6455	2.1650
O6	3.8478	−1.3737	2.1650
Al3	0.0000	−2.7474	3.0076
Al4	2.3793	−1.3737	3.4873

[a]Positive z values correspond to displacements into the bulk. Atom labels correspond to those used in Fig. 5.

theoretical beams had to be averaged before comparison with experiment.

For each of our reference surface terminations, we used the latest TLEED codes [9] to compute theoretical LEED intensities. These were compared with the experimental values in a directed search using the Pendry R-factor [19] in which the coordinates of all the atoms and the inner potential were allowed to vary. The TLEED formalism is an approximation that is accurate for atomic movements of the order of 0.4 Å. If the best-fit structure was found to show atom movements of this order, the original reference structure was changed and the calculation repeated. This procedure helps to avoid the calculations becoming stuck in false minima.

6. Results

6.1. Single termination surfaces

The result of the TLEED calculations for the Al-bilayer (B) structure produced R-factors $R>0.7$ for any reasonable displacements from the original reference structure. As Pendry R-factors of less than 0.5 are normal for a moderate or better agreement of theory and experimental values, this structure was not pursued further. The R-factors for the TLEED optimized O-terminated (A) and Al-terminated (C) structures gave similar

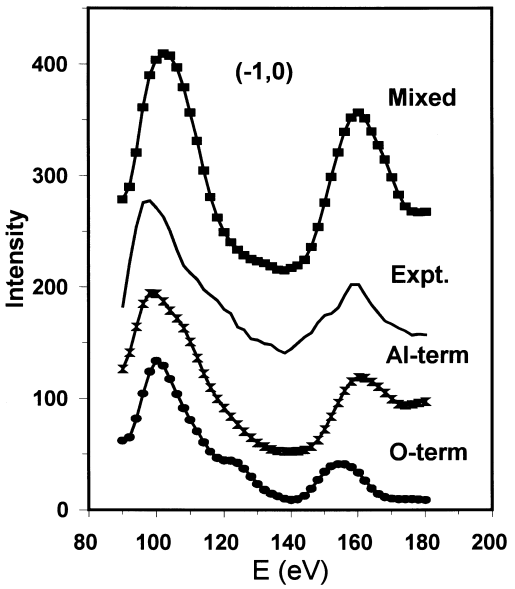

Fig. 11. Comparison of experimental $I(V)$ curves for the averaged $(\bar{1}0)$ beam from (0001) alumina with the results of the optimized TLEED calculation for an Al-terminated, O-terminated surface and a mixture of the two terminations.

mediocre R-factors of 0.42 and 0.43, respectively. Representative examples of the fit of experiment and theory for the averaged $(\bar{1}0)$ beam from the single termination structures are shown as part of Fig. 11.

The atomic displacements for the A-reference structure (O-terminated) are shown in Table 2. The movements are all relatively small. Here, the top set of O layers has moved out about 0.06 Å and twisted laterally. The Al atoms in the first bilayer (Al 1/2) have moved closer to coplanarity. The movements in deeper layers are all less than 0.1 A. The atomic displacements for the C-reference structure (Al-terminated) shown in Table 3 indicate that the topmost Al2 layer has moved about 0.1 Å outward from the triplet of O atoms below it, increasing the spacing between these two layers to about 0.96 Å. Atoms Al3 and Al4 have become closer to coplanar, whereas the O1–3 triplet has twisted laterally.

6.2. Surfaces with mixed terminations

The similar mediocre level of agreement of either the Al- or O-terminated single termination struc-

Table 2
The optimized TLEED structure for alumina (0001) starting from the O-terminated reference structure A given as displacements from the initial coordinates of Table 1[a]

O-terminated (A): $RP=0.42$, $V_{or}=20.6$ eV			
Atom	Δx (Å)	Δx (Å)	Δz (Å)
O1	−0.142	0.030	−0.062
O2	0.047	−0.138	−0.062
O3	0.096	0.109	−0.062
Al1	0.000	0.000	0.010
Al2	0.000	0.000	−0.112
O4	0.070	−0.049	0.004
O5	−0.007	0.085	0.004
O6	−0.077	−0.036	0.004
Al3	0.000	0.000	0.027
Al4	0.000	0.000	0.005

[a]Positive z displacements (Δz) correspond to displacements into the bulk. Atom labels correspond to those used in Fig. 5.

Table 3
The optimized TLEED structure for alumina (0001) starting from the Al-terminated reference structure C given as displacements from the initial coordinates of Table 1[a]

Al-terminated (C): $RP=0.42$, $V_{or}=20.0$ eV			
Atom	Δx (Å)	Δy (Å)	Δz (Å)
Al1	0.000	0.000	−0.127
O1	−0.237	−0.002	−0.034
O2	0.117	−0.198	−0.034
O3	0.121	0.204	−0.034
Al2	0.000	0.000	0.059
Al3	0.000	0.000	−0.192

[a]Positive z displacements (Δz) correspond to displacements into the bulk. Atom labels correspond to those used in Fig. 5.

tures indicates that perhaps a mixture of terminations is occurring. Starting from the optimized single domain O-terminated structure, the *R*-factor drops sharply as small amounts of the Al-terminated surface are included (Fig. 12). The *R*-factor continues to drop until it reaches a minimum value of 0.26 at a 2:1 O/Al-terminated surface weighting. Increasing the amount of Al-terminated surface beyond this value leads to an increase in the *R*-factor back towards the all Al-terminated value of 0.42. However, the *R*-factor remains at very good values of 0.26–0.28 for Al/O ratios as low as 0.25 to values as high as 1.0, so the best-fit

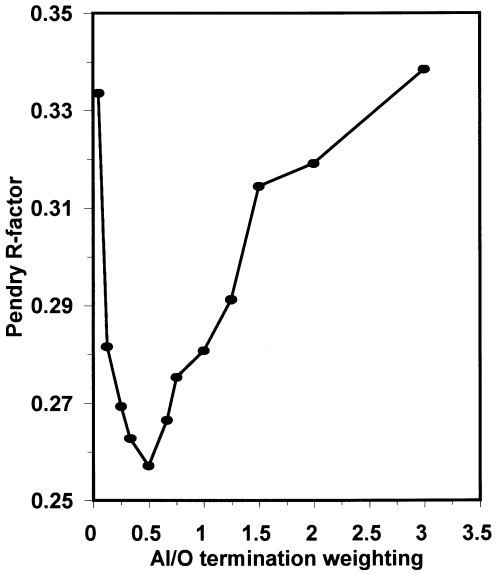

Fig. 12. Variation of the Pendry *R*-factor for TLEED calculations for (0001) alumina with the weighting ratio Al/O for a mixture of Al and O-terminated domains.

value of Al/O = 0.5 may depend upon the step distribution.

For this mixed structure, all the diffracted beams give good individual *R*-factors, the largest being 0.34. Fig. 11 shows how the fit of the $(\bar{1},0)$ beam seen already for single-termination structures changes for the mixed termination surface. The changes are subtle and underscore the need for an *R*-factor analysis that includes many beams. Other examples of the fit for a 2:1 O/Al weighted surface are shown in Fig. 13. Here, we show the fit to the experiment for beams that have various levels of agreement. The $(1\bar{2})$ beam shows a very good agreement with $RP=0.22$. The (00) beam appears to the eye to fit less well than the $(1\bar{2})$ and has a higher $RP=0.26$. The $(\bar{2}0)$ beam appears to fit very well to the experiment but has a relatively poor value of $RP=0.34$. The contradiction between the optical and *R*-factor fits for the (00) and $(\bar{2}0)$ beams may be due to the higher noise level in the $(\bar{2}0)$ beam.

The final coordinates of atoms in Al and O-terminated regions of the 2:1 mixed surface model are gathered in Table 4. Atom movements are generally less than 0.3 Å. In the Al-terminated

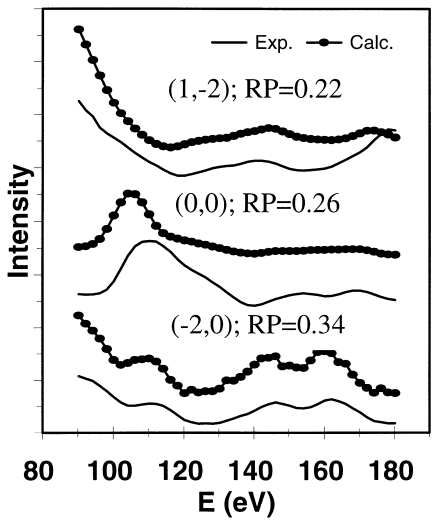

Fig. 13. Comparison of experimental $I(V)$ curves for the averaged $(1\bar{2})$, (00) and $(\bar{2}0)$ beams from (0001) alumina with the results of the optimized TLEED calculation for a mixture of Al and O-terminated domains.

Table 4
The optimized TLEED structure for alumina (0001) for 2:1 mixed domains of O-terminated reference structure A and Al-terminated reference structure C given as displacements from the initial coordinates of Table 1[a]

2:1 mixture O- (A) and Al-terminated (C): $RP=0.26$, $V_{or}=19.2$ eV			
Atom	Δx (Å)	Δy (Å)	Δz (Å)
O-terminated domain			
O1	−0.170	0.028	−0.123
O2	0.061	−0.161	−0.123
O3	0.109	0.133	−0.123
Al1	0.000	0.000	−0.099
Al2	0.000	0.000	−0.110
O4	0.286	0.207	−0.006
O5	−0.322	0.144	−0.006
O6	0.036	−0.351	−0.006
Al3	0.000	0.000	−0.020
Al4	0.000	0.000	−0.069
Al-terminated domain			
Al1	0.000	0.000	−0.203
O1	−0.271	0.077	0.045
O2	0.069	−0.273	0.045
O3	0.202	0.196	0.045
Al2	0.000	0.000	−0.001
Al3	0.000	0.000	0.273

[a]Positive z displacements correspond to displacements into the bulk. Atom labels correspond to those used in Fig. 5.

region, the topmost Al atom has moved out from the underlying oxygen layer, in which the O 1–3 atoms have twisted clockwise. In the next Al bilayer, the Al atoms have separated somewhat. In the O-terminated region, the topmost O and Al atom layers have also moved outwards compared to the reference structure. The lower O atom layers have very small shifts in the normal direction. The O atoms in this region all show some twists in the (x, y) plane. A consideration of the variation of the R-factor as a function of the displacement away from the minimum R-factor structure shows that the sensitivity to changes in atom positions varies markedly from atom to atom. In both the O- and Al-terminated regions, the sensitivity to small structural changes is, as expected, greatest for those atoms closest to the surface and in the normal direction. Moving the topmost atoms in both regions as little as 0.1 Å increases the R-factor by 0.1. However, movement of atoms in the bottom layers of the surface structure by the same amount leads to R-factor increases of 0.02 or less. If we assume that the R-factor must change by at least 0.05 to be a significant change, then we can expect that the final coordinates of the topmost atoms are correct to 0.05 Å, but the coordinates of atoms in lower layers may well be in error by as much as 0.1 Å. The optimized inner potential shifts only very slightly to 19.2 eV.

7. Discussion

A number of theoretical investigations of the alumina (0001) surface have appeared in the literature [5–8]. The usual approach in these studies is to cleave an alumina crystal to produce one of the terminations A–C used here and minimize the energy of the system. Inherent in this process is the production of a second cleavage surface. Only one type of cleavage produces two identical surfaces – that which results in a C-termination with a single surface Al layer. Other cleavages produce mixtures of A and B-type termination on the two cleavage planes. Local-density calculations [6] predict the Al-terminated C surface to be the most stable. Only this surface is autocompensated [20] – that is chemically stable and charge-neutral. As a result, theorists

Table 5
Theoretical predictions of the normal relaxation Δz_1 (Å) of the outer Al layer of an Al-terminated C structure for alumina (0001)[a]

Theoretical method	Δz_1 (Å)	Reference
Hartree-Fock	−0.4	[5]
Local density	0.1	[6]
Pseudopotentials	−0.7	[7]
Tight-binding	−0.7	[8]

[a]Negative values of Δz_1 correspond to a contraction of the top interlayer spacing relative to an unrelaxed surface.

have concentrated on this surface. The results, shown in Table 5, uniformly predict a contraction of the top Al layer by 0.4–0.7 Å. Contraction of the latter magnitude results in an almost coplanar Al–O surface layer and tends to minimize the classical electric dipole moment of the top atomic layers.

Clearly, the theoretical predictions of a contracted Al-terminated surface are at odds with our result. However, these calculations do not consider the same surface as that used in our experiment. Theory assumes that the alumina crystal has been cleaved in vacuo to produce the most stable pair of (0001) surfaces. Whereas this is a theoretically desirable approach, the reality is that alumina crystals cannot be cleaved along (0001). Weiderhorn [21] found that he could not produce a (0001) fracture surface because the crack propagated along lower energy fracture surfaces instead of (0001).

It is difficult to visualize an experiment that would accurately mimic the fracture conditions envisaged in the theoretical investigations. As fracture surfaces of alumina (0001) cannot be prepared experimentally, the only surface accessible to the experiment is that prepared using the cleaning procedures that we employed. Thus, our experiments address the structure of a real alumina surface, whereas theoretical investigations have used unrealistic surfaces. Our results further indicate that some expansion of surface layers occurs in both O- and Al-terminated surfaces. Theory predicts that considerable contractions up to 0.4–0.7 Å occur in Al-terminated surfaces. We found that contractions of these magnitudes showed a poorer agreement with experimental data.

The good agreement between the calculations and the experiment gives us confidence that a mixed O/Al-terminated surface is the correct description of this surface. It is possible that the surface is actually a more complex structure than that derived from these simple model reference structures, although any reconstruction must preserve the (1×1) symmetry. Information from other experimental techniques such as atomic force microscopy or ion scattering would be useful to confirm our structure.

8. Conclusion

A tensor LEED determination of the (0001) surface of α-Al_2O_3 produced by oxygen cleaning/annealing cycles indicates that surfaces with a single type of atom termination give only mediocre agreement with experiment. A mixture of Al and O-terminated domains gives good agreement (Pendry R-factor = 0.26) with experiment. Our data indicate that in either case, the outermost atomic layer relaxes outward, with some twisting and relief of buckling in deeper layers. An outward relaxation of the top layer is in disagreement with theoretical predictions. However, such predictions are for vacuum-cleaved surfaces that are not realistic models for the surface obtained in our experiment.

Acknowledgements

We would like to thank Dr Michel Van Hove (LBL) for assistance with the TLEED codes and Prof. Arthur Sleight and Dr Matthews Hall (OSU) for providing the facilities for Ta sputtering.

References

[1] J.M. Charig, Appl. Phys. Lett. 10 (1967) 139.
[2] C.C. Chang, Appl. Phys. 39 (1968) 5570.
[3] T.M. French, G.A. Somorjai, J. Phys. Chem. 74 (1970) 2489.

[4] P.S.P. Wei, A.W. Smith, J. Vac. Sci. Technol. 9 (1972) 1209.
[5] M. Causa, R. Dovesi, C. Pisani, C. Roetti, Surf. Sci. 215 (1989) 259.
[6] I. Manassidis, A. De Vita, M.J. Gillan, Surf. Sci. 285 (1993) L517.
[7] J. Guo, D.E. Ellis, D.J. Lam, Phys. Rev. B 45 (1992) 13647.
[8] T.J. Godin, J.P. La Femina, Phys. Rev. B 49 (1994) 7691.
[9] M.A. Van Hove, Off-normal Automated Tensor LEED, Lawrence Berkeley Laboratory, Berkeley, CA.
[10] N.F.M. Henry, K.K. Lonsdale, International Tables for X-ray Crystallography, The Kynoch Press, Edinburgh, 1952.
[11] P. Thompson, D.E. Cox, J.B. Hastings, J. Appl. Cryst. 20 (1987) 79.
[12] P.R. Watson, M.A. Van Hove, K. Hermann, NIST Surface Structure Database V2.0, National Institute of Standards and Technology, Gaithersburg, MD, 1996.
[13] N.J. Tro, S.M. George, Surf. Sci. 197 (1988) L246.
[14] D.R. Haynes, K.R. Helwig, N.J. Tro, S.M. George, J. Chem. Phys. 93 (1990) 2836.
[15] H. Pappa, D. Moorhead, K. Heinemann, Thin Solid Films 128 (1985) 251.
[16] S.L. Cunningham, W.H. Weinberg, Rev. Sci. Instrum. 49 (1978) 7.
[17] J. Toofan, P.R. Watson, Rev. Sci. Instrum. 65 (1994) 3382.
[18] K. Schwarz, Phys. Rev. B 5 (1972) 2466.
[19] J.B. Pendry, J. Phys. C 13 (1980) 937.
[20] W.A. Harrison, J. Vac. Sci. Technol. A 16 (1979) 1492.
[21] S.M. Wiederhorn, J. Am. Ceram. Soc. 52 (1969) 485.